Received: 20 February 2022 | Revised: 5 November 2022 | Accepted: 17 November 2022

DOI: 10.1002/mgg3.2119

Molecular Genetics & Genomic Medicine Open Access WILEY

ORIGINAL ARTICLE

A novel mutation in the collagen domain of EDA results in hypohidrotic ectodermal dysplasia by impacting the receptor-binding capability

Xingyu Liu | **Yuming Zhao** | **Junxia Zhu**

Department of Pediatric Dentistry, Peking University School and Hospital of Stomatology & National Center of Stomatology & National Clinical Research Center for Oral Diseases & National Engineering Laboratory for Digital and Material Technology of Stomatology & Central Laboratory, Peking University School and Hospital of Stomatology, Beijing, China

Correspondence
Junxia Zhu, Department of Pediatric Dentistry, Peking University School and Hospital of Stomatology & National Center of Stomatology & National Clinical Research Center for Oral Diseases & National Engineering Laboratory for Digital and Material Technology of Stomatology & Central Laboratory, Peking University School and Hospital of Stomatology, No. 22, Zhongguancun South Avenue, Haidian District, Beijing 100081, PR China.
Email: zhujxsmile@163.com

Funding information
National Natural Science Foundation of China, Grant/Award Number: 81500828

Abstract

Background: Hypohidrotic ectodermal dysplasia (HED) mainly results from gene mutations in the EDA/EDAR/NF-κB pathway. Function analysis of the mutations in the collagen domain of ectodysplasin A (EDA)result in HED has been rarely studied. This study aimed at determining the mechanism by which the novel collagen domain mutation of EDA results in HED.

Methods: We analyzed the DNAs from a Chinese family with HED and performed bioinformatics analysis. A new three-dimensional structure model of the EDA trimer was built and used to predict the effect of the mutations on EDA. We performed a western blot to detect EDA1 proteins in cell lysates and supernatants. We then performed coimmunoprecipitation to determine whether the mutation would affect the interaction of EDA1 with the EDA receptor (EDAR). Dual luciferase reporter assay and immunofluorescence were performed to detect the effect of the mutant EDA1 protein on nuclear factor kappa B (NF-κB) activation.

Results: A novel missense mutation (c.593G > A, p. Gly198Glu) in the collagen domain of EDA was detected. The mutation was predicted to be disease-causing. A three-dimensional structure model of the EDA trimer was first built in this study, in which the mutation site is located around the receptor binding domain. Functional studies showed that there was no difference in the secretion activity between the mutant EDA1 and the wild-type EDA1. However, the receptor-binding activity and the transcription activation of NF-κB were impaired by the mutation.

Conclusion: We identified a novel mutation (c.593G > A, p. Gly198Glu) in the collagen domain of EDA. Bioinformatics analysis and functional studies showed this mutation was damaging, indicating that mutations in the collagen domain of EDA could result in HED by affecting the receptor-binding activity of EDA and the transcriptional activity of NF-κB.

KEYWORDS
collagen domain, EDA, hypohidrotic ectodermal dysplasia, NF-κB

1 | INTRODUCTION

Ectodermal dysplasia (ED, MIM: 305100) refers to a group of inherited disorders with abnormal development of two or more ectoderm structures, such as hair, teeth, nails, and sweat glands (Visinoni et al., 2009; Wohlfart et al., 2016). Hypohidrotic ectodermal dysplasia (HED) characterized by hypotrichosis, hypohidrosis, and hypodontia is the most common form of ED (Cluzeau et al., 2011; Keller et al., 2011). Tissues and organs derived from the ectoderm are developed from placodes. As the signaling center of embryonic development, placodes express signaling molecules of the WNT signaling pathway, the Hedgehog signaling pathway, the fibroblast growth factor (FGF) family, the transforming growth factor-beta (TGF-β) family, and the TNF family (Norderyd, 2012). HED mainly results from gene mutations in TNF-α and related pathways, especially the EDA/EDAR/NF-κB pathway (Cluzeau et al., 2011).

Mutations of many genes in the EDA/EDAR/NF-κB pathway result in HED, which interferes with epithelium-mesenchymal interactions and gives rise to developmental anomalies and dysmorphogenesis of ectodermal structures (Cui & Schlessinger, 2006). Mutations of the *EDA* gene (MIM: 300451) have been detected in more than 50% of reported HED cases (Cluzeau et al., 2011; Martinez-Romero et al., 2019). EDA1 (391 aa) and EDA2 (389 aa) are the only two isoforms of EDA containing a TNF homology domain (THD) as a receptor-binding site. EDA1 binds to EDAR, while EDA2 binds to XEDAR. As a member of the TNF family, EDA consists of several functional domains, including the transmembrane domain, the Furin cleavage site, the collagen domain, and the THD (Cui & Schlessinger, 2006). Functional analyses were performed to reveal the pathogenic mechanism of HED. Previous functional studies mainly focus on THD and Furin cleavage site, while the mechanism by which the mutations in the collagen domain result in hypohidrotic ectodermal dysplasia has been rarely studied.

A proteolytically processed homotrimer form is essential for EDA to bind receptors and then activate downstream pathways. The collagen domain contains a $(Gly\text{-}X\text{-}Y)_{19}$ collagen-like repeat. It was hypothesized that the collagen triple helix yielded a multimeric protein through assembly into an N-terminal bundle structure (Kishore & Reid, 1999), which induced the multimerization of the TNF homology region. Furthermore, the multimerization of EDA could be disrupted by point mutations in the collagen domain rather than in-frame deletions (Schneider et al., 2001). However, the position of the collagen domain in EDA protein conformation and how mutations in the collagen domain cause HED are still uncertain.

In this study, we described the clinical features and molecular characterizations of a novel mutation in the collagen domain of *EDA* identified in a Chinese family with HED. We performed three-dimensional protein structure prediction and functional studies to explore the molecular mechanisms underlying the effects of mutations in the collagen domain of EDA.

2 | PATIENTS AND METHODS

2.1 | Subjects

The proband was an 8-year-old boy referred to Peking University School and Hospital of Stomatology for his oligodontia condition. He showed mild hypohidrosis with obvious heat intolerance, proneness to eczema, and difficulty eating. His mother and sisters also had hypodontia. Clinical examination showed short stature, sparse hair and eyebrows, and periorbital hyperpigmentation. His skin was soft and dry and showed desquamation and crusting. He also showed facial features, including frontal bossing, chin prominence, maxillary hypoplasia, and protuberant lips. Intraoral examination revealed anodontia and a lack of alveolar bone development. The phenotypic features of the proband are shown in Figure 1.

2.2 | Mutation detection

Peripheral blood was collected from the proband and his family. A TIANamp Blood DNA Kit (Tiangen Biotech, Beijing, China) was used for the extraction of genomic DNA according to the manufacturer's instructions. We selected the proband for whole-exome sequencing. After target enrichment and library preparations, 100-base paired-end reads were generated and sequenced by combinatorial probe-anchor synthesis (cPAS) on the BGISEQ-500 platform (BGI-Shenzhen, China). The proband was sequenced to a mean depth of 94.30X, and approximately 98.87% of the target region was covered by 10 or more reads.

First, all of the non-coding and synonymous variants were removed. Then, all candidate variants were filtered according to minor allele frequency against public databases, including the 1000 Genomes Project, the Single Nucleotide Polymorphism Database (dbSNP), and the NHLBI exome sequencing project (ESP) 6500. Finally, we focused the analysis on known HED-related genes, including *EDA* (NM_001399.5), *EDAR*, *EDARADD*, *TRAF*, *NEMO*, and *WNT10A*. The variant-encompassing region was amplified by polymerase chain reaction (PCR) using specific primers as described

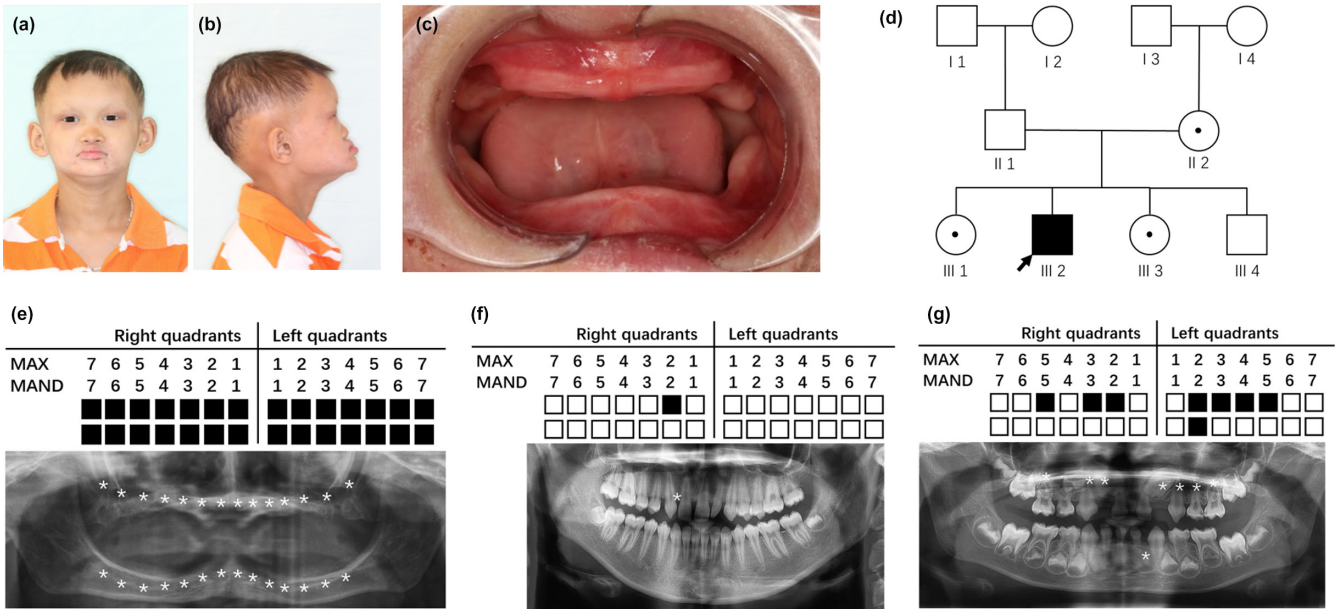

FIGURE 1 Phenotypic features of members of the pedigree. (a and b) Photograph of the proband showing facial features including frontal bossing, chin prominence, maxillary hypoplasia, protuberant lips, sparse hair and eyebrows, and periorbital hyperpigmentation. (c and e) Intraoral photograph and panoramic radiograph of the proband showing anodontia and a lack of alveolar bone development. (d) Pedigree chart of the family. The affected individual is represented by filled squares (male), while carriers are represented by circles with a vertical line (females). (f and g) Panoramic radiograph of the elder sister and younger sister of the proband showing the reduced number of permanent teeth.

previously (Fan et al., 2008). Then, Sanger sequencing of all individuals in this family was performed to validate the candidate variant, and the sequences were analyzed using Chromas chromatogram viewer (http://technelysium.com.au/wp/chromas/).

2.3 | Bioinformatics study and structural modeling

The prediction tools MutationTaster (http://www.mutationtaster.org/), PolyPhen2 (http://genetics.bwh.harvard.edu/pph2/), Sorting Intolerant from Tolerant (SIFT) (https://sift.bii.a-star.edu.sg/), and CADD (https://cadd.gs.washington.edu/score/) were used to estimate the likelihood that an amino acid transition may affect the function of the protein. In addition, the secondary structures of wild-type EDA1 and mutant EDA1 were predicted by PSIPRED 4.0 (http://bioinf.cs.ucl.ac.uk/psipred/).

The three-dimensional (3D) structures of wild-type and mutant EDA1 were modeled and visualized with PyMOL2.0 (The PyMOL Molecular Graphics System, Version 2.0 Schrödinger, LLC). We aligned the EDA1 monomer structure predicted by the AlphaFold Protein Structure Database (https://alphafold.ebi.ac.uk/) with the crystal structure of the EDA1 trimer (PDB ID 1RJ7; X-ray, resolution 2.3 Å) for modeling.

2.4 | Construction of EDA1 expression vectors

Mammalian vectors pcDNA3.1 were used to construct expression vectors for secreted wild-type EDA1 and mutant EDA1 with p.Gly198Glu (G198E) and p.Gly198Ala (G198A). Mutant EDA1 with p.His252Leu (H252L) and p.Ser374Arg (S374R) (Schneider et al., 2001) were also constructed to make a contrast as HED-causing mutation and non-syndromic tooth agenesis-causing mutation, respectively. The expression vector sequence is composed of an HA signal peptide, a FLAG tag, a linker (GGACC CGGACAGGTGCAGCTGCAG GTCGACGAAAATCAG), and the coding sequence of all the amino acids of EDA1. Expression vectors for EDAR:Fc were constructed with a sequence including an Fc tag and all the amino acids of EDAR. All the above expression vectors were constructed and verified using direct sequencing by GENEWIZ, Suzhou, China.

2.5 | Expression of soluble EDA1 in cells and supernatants

The abovementioned vectors were transfected into human embryonic kidney 293T (HEK293T) cells using Lipofectamine 3000 (Invitrogen Corporation, Carlsbad, CA, USA), and then the cells were maintained in

serum-free OptiMEM (Invitrogen Corporation, Carlsbad, CA, USA) culture medium for 48 h. Then, the EDA1 proteins in cell lysates and supernatants were collected separately and detected by anti-EDA (Abcam, Shanghai, China) western blot.

2.6 | Coimmunoprecipitation assay

Receptor EDAR: Fc (~500 μg in 200–500 μl of cell lysates) was added to 20–30 μl protein G agarose (Beyotime Institute of Biotechnology, Beijing, China), mixed with EDA1 proteins (~1 mg in 200–500 μl of cell supernatants) and incubated on a rotating wheel overnight at 4°C. Protein G agarose was washed three times with 1 ml PBS after centrifugation at 3000 rpm for 5 min at 4°C. An equal volume of 2× sodium dodecyl sulfate (SDS) loading buffer was added to Protein G agarose for resuspension and boiled for 10 min. Samples were analyzed by western blot with an anti-EDA antibody (Abcam, Shanghai, China) and an anti-Fc antibody (Abcam, Shanghai, China) for western blot analysis. Each experiment was repeated three times.

2.7 | Luciferase reporter assay

Three plasmids (pNF-κB-luc plasmid, EDA1 mutant plasmid, and pRL-TK plasmid) were cotransfected into mouse ameloblast-derived LS8 cells (Chen et al., 1992). The pcDNA3.1 vector was used as a negative control, while the wild-type EDA1 vector was used as a positive control. After culturing for 48 hours, a dual luciferase assay system (Promega Corporation, Madison, WI, USA) was used to measure the firefly and Renilla luciferase activities with a Synergy 2 Multi-Detection Microplate Reader (BioTek, Winooski, VT, USA). Firefly luciferase activity was normalized to Renilla luciferase activity. All experiments were performed in triplicate, and each experiment was repeated three times. The results were assessed for statistical significance using the Student's *t* test and analysis of variance.

2.8 | Immunofluorescence

The pcDNA3.1 vector and wild-type or mutant vectors described before were transfected into LS8 cells. Immunofluorescence was performed using a primary antibody against NF-κB p65 (Abcam, Shanghai, China). Goat anti-rabbit IgG/RBITC (Solarbio, Beijing, China) was used for detection. Slides were mounted with mounting medium, antifaded with DAPI (Solarbio, Beijing, China), and imaged by fluorescence microscopy.

3 | RESULTS

3.1 | Identification and bioinformatics study of mutations in the *EDA* gene

Out of the 21,765 variants identified by WES, 6 nonsynonymous variants occurred in known HED-related genes (*EDA*, *EDAR*, *EDARADD*, *WNT10A*, *NEMO*, and *TRAF6*). After removing common variants with MAF>0.01, we identified a novel missense mutation p.Gly198Glu (c.593 T > A) in *EDA*. The variant was further confirmed by Sanger sequencing and was carried by the proband's mother and sisters (Figure 2b,c,e). The variant was predicted to be damaging by Mutation Taster, PolyPhen2, and SIFT with a CADD score of 25.8. The site of the variant is highly conserved among human, chimpanzee, rhesus, horse, bovine, dog, rabbit, rat, and mouse protein sequences (Figure 2f). In 2002, a de novo mutation in this site p.Gly198Ala (c.593G > C) was reported in a French boy with XLHED, and no functional studies were performed.

3.2 | The collagen domain closely surrounds the THD in the EDA1 trimer

The secondary structure prediction of the EDA1 protein by PsiPred showed that residue Gly198 was located in a coil structure, and the mutation p.Gly198Glu could affect the secondary structure of the protein. By aligning the monomer structure predicted by AlphaFold (Figure 3a–c) to the known model PDB ID: 1RJ7, we built a new three-dimensional structure of the EDA1 trimer. Residue Gly198 and the collagen domain (180–235 aa) closely surround the THD (Figure 3d–f). The nonpolar Ala residue has a methyl for its side chain (Figure 3h), while the negatively charged hydrophilic Glu residue has a γ-carboxyl instead of a hydrogen atom of the hydrophobic Gly residue (Figure 3g,i). Thus, the side chain volume and polarity with hydrophobic interactions of the residue changed when the two mutations p.Gly198Ala and p.Gly198Glu occurred, which could impair the stability of the EDA1 trimer.

3.3 | The p.Gly198Glu and p.Gly198Ala mutations affect the receptor-binding capability of EDA1

The mutation p.Gly198Glu identified in this study and the same site mutation p.Gly198Ala with pathogenic mutations p.His252Leu and p.Ser374Arg were tested for the expression and receptor-binding capability. The results showed that all the wild-type and mutant EDA1 could

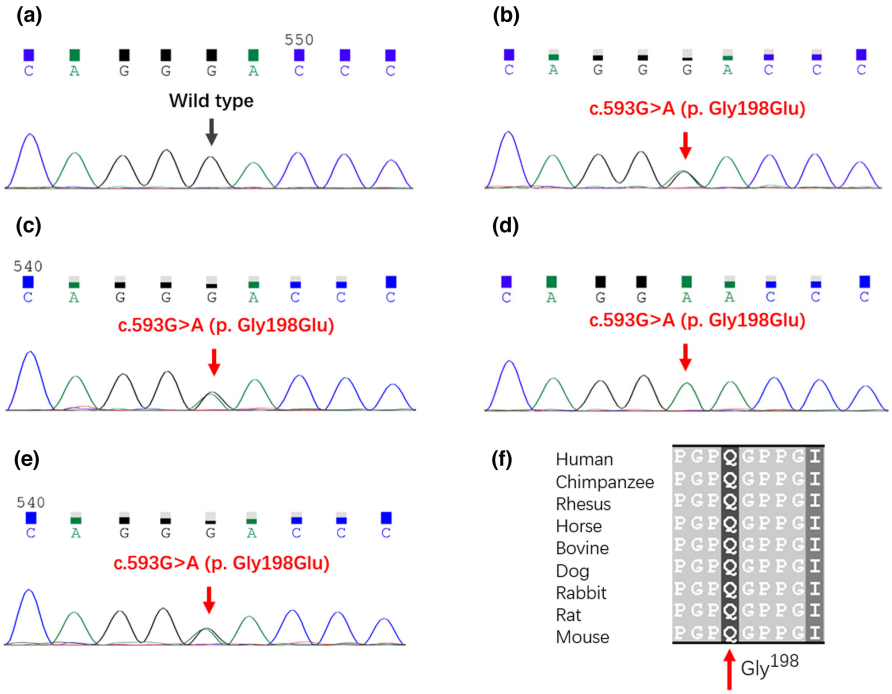

FIGURE 2 Mutation detection of members of the pedigree. (a) Sequencing chromatogram of the unaffected father. (b, c, and e) Sequencing chromatogram of the heterozygous mutation c.593G > A in the *EDA* gene of the female carriers. (d) Sequencing chromatogram of the missense mutation c.593G > A in the *EDA* gene of the proband. (f) Sequence alignment results show that residue Gly198 is conserved across nine species. The mutant allele is marked by the red arrow.

be expressed in both the cell lysates and supernatants (Figure 4a), which indicated that mutants affecting the collagen domain could be expressed as soluble secreted proteins. Coimmunoprecipitation was performed to detect the receptor-binding ability of the mutant proteins. As described before, EDA1 p.His252Leu lost almost all the ability, and EDA1 p.Ser374Arg lost the partial ability to interact with EDAR. EDA1 p.Gly198Glu and EDA1 p.Gly198Ala both displayed weaker binding to EDAR than wild-type EDA1 (Figure 4b).

3.4 | The p.Gly198Glu and p.Gly198Ala mutations impair the transcriptional activation of NF-κB

The EDA/EDAR/NF-κB signaling pathway plays an important role in the development of ectodermal appendages. Regarding tooth development, EDA is expressed in the dental epithelium. LS8, an epithelium-derived ameloblast cell line that has been proven to express EDAR (Shen et al., 2016), was used in this study to detect the activation of the EDA/EDAR/NF-κB signaling pathway. The receptor-binding capability of p.Gly198Glu and p.Gly198Ala mutant proteins was only partially impaired, but the impact of this impaired binding on the downstream NF-κB pathway remained unknown. When the NF-κB pathway is activated, its component p65 transfer into the cell nucleus. Thus, immunofluorescence and dual luciferase assays of NF-κB submitted to p65 were performed.

According to the immunofluorescence results, the red fluorescence of p65 was more intense and gathered more at nucleoli in wild-type EDA1-transfected LS8 cells than in pcDNA3.1-transfected LS8 cells. However, the nuclear expression of p65 decreased in p.Gly198Glu-, p.Gly198Ala-, and p.His252Leu mutant EDA1-transfected LS8 cells, and no nucleolar aggregation could be detected. In some p.Ser374Arg mutant EDA1-transfected LS8 cells, we observed nuclear expression and nucleolar aggregation (Figure 5a–r). As known disease-caused mutations, we found p.His252Leu and p.Ser374Arg interfered the transfer of p65 toward the nucleus and the transcriptional activity of NF-κB, which is consistent with previous literature. The dual-luciferase assay results showed that there was a significant difference in the transcriptional activation of p65 between all the mutant EDA1- and wild-type EDA1-transfected LS8 cells, and the activation was higher in the p.Ser374Arg mutant EDA1-transfected LS8 cells than in the other mutant EDA1-transfected LS8 cells, which supported the immunofluorescence results (Figure 5s). Taken together, these results indicated that p.Gly198Glu and p.Gly198Ala mutant EDA1 reduced the activation of the NF-κB pathway in LS8 cells.

4 | DISCUSSION

X-linked HED (XLHED) caused by mutations in the *EDA* gene is the most frequent form of HED (Cluzeau et al., 2011; Keller et al., 2011). There are only 20 reported mutations in the collagen domain of EDA among all 176 reported *EDA* point mutations according to the public Human Gene Mutation Database, and few of them have been studied by functional analysis. In this study, we

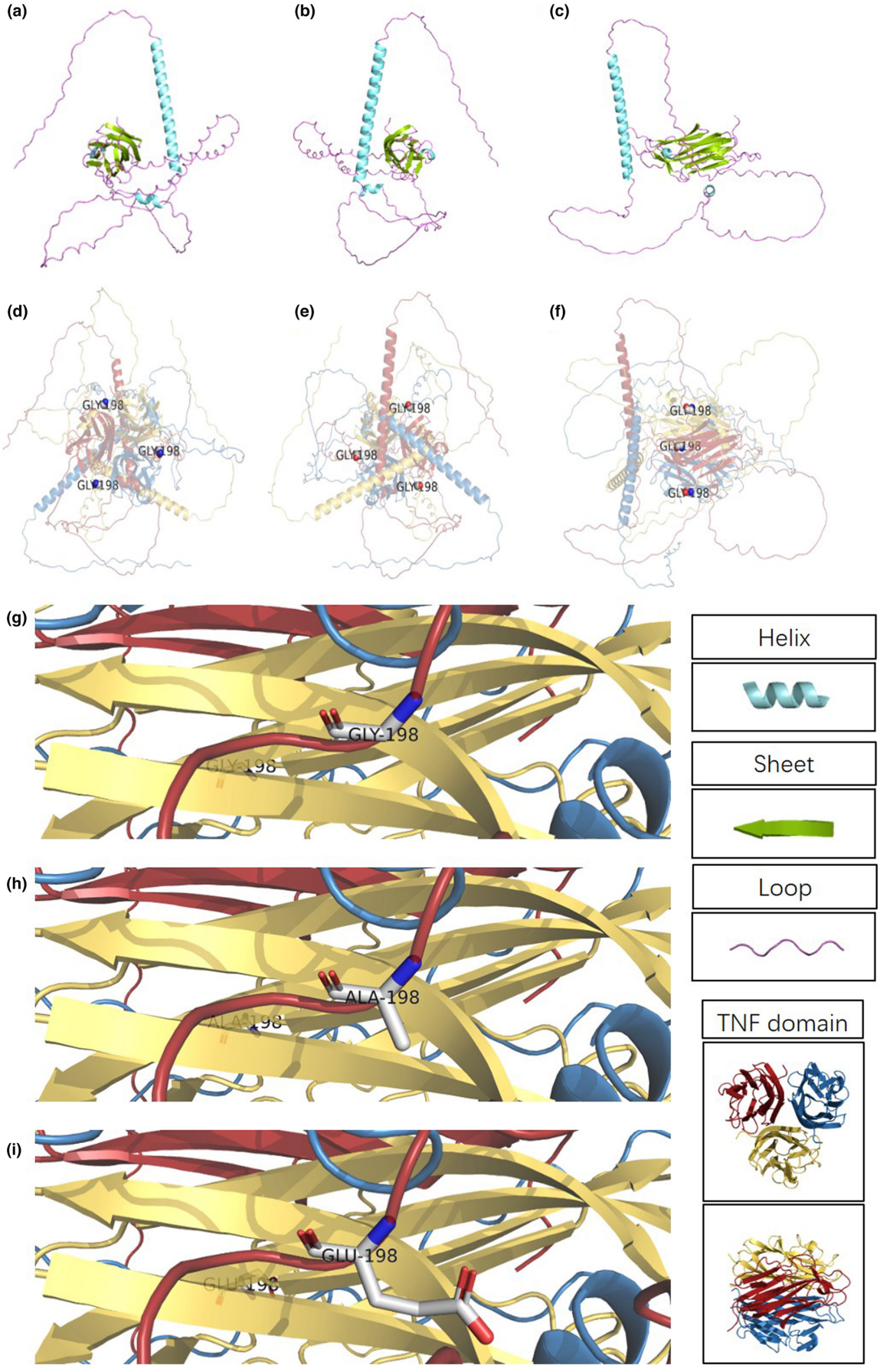

FIGURE 3 Three-dimensional structure prediction of the EDA1 trimer. (a–c) The monomer structure of EDA1 predicted by AlphaFold. (d–f) Residue Gly198 closely surrounds the THD in the new three-dimensional structure of the EDA1 trimer. (g and h) The negatively charged hydrophilic Glu residue has a γ-carboxyl group instead of a hydrogen atom of the hydrophobic Gly residue.

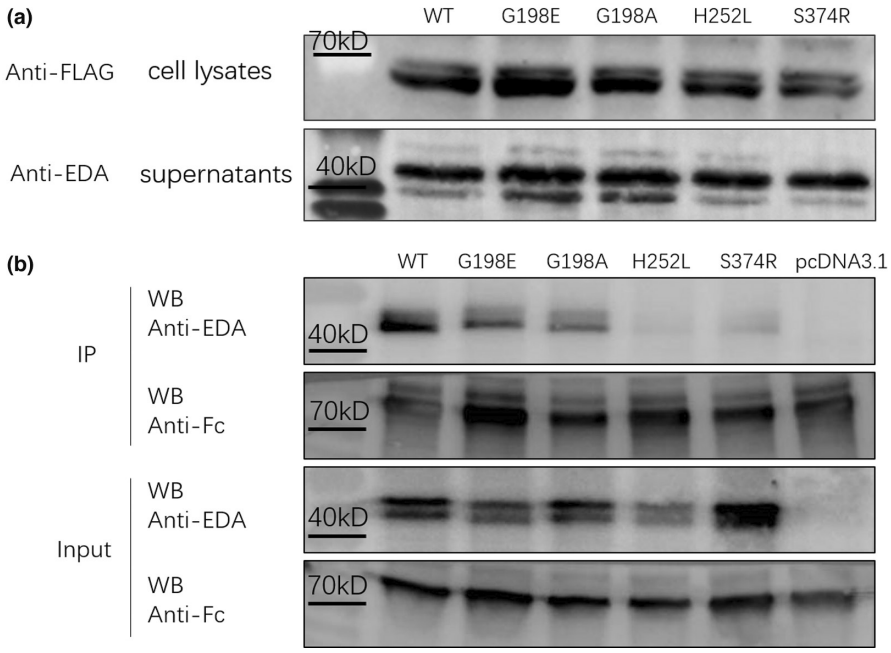

FIGURE 4 Expression and receptor binding ability of wild-type and mutant EDA1 proteins. (a) Western blots depicting the expression of wild-type and mutant EDA1 in the cell lysate and supernatant of transfected HEK293T cells. (b) EDA1 in supernatants was immunoprecipitated with EDAR:Fc, and western blots revealed that p.Gly198Glu EDA1 showed a decreased receptor binding ability.

identified a novel collagen domain mutation p.Gly198Glu in a Chinese XLHED family. The proband showed a typical phenotype of HED characterized by hypotrichosis, hypohidrosis, and hypodontia with some facial features. The mother and two sisters showed only defective dentition without hypotrichosis or hypohidrosis, which is consistent with the mild phenotype in female carriers (Reyes-Reali et al., 2018). Interestingly, there is a clear distinction between the number of missing teeth of the two sisters, indicating that the phenotype is not only determined by gene mutations but also by the penetrance and expressivity of genes, as well as a potential effect of genetic modifiers (Rahit & Tarailo-Graovac, 2020; Reyes-Reali et al., 2018).

The p.Gly198Glu mutation was predicted to be disease-causing and change the secondary structure of EDA. The results of immunofluorescence and dual luciferase assays of NF-κB were powerful support for the bioinformatic prediction. As far as we know, the previous three-dimensional model of EDA covered only the THD (Mues et al., 2010; Wang et al., 2020; Zeng et al., 2015), which was built up according to the crystal structure of EDA1 determined by X-ray diffraction. During this year, the AlphaFold Protein Structure Database released structures of the ~20,000 known proteins expressed in the human body, including the monomer structure of EDA. By aligning these two models, we built the first model of a bioactive trimeric EDA. On the basis of this model, the protein structure prediction after various mutations for the bioactive form of EDA could be performed. The three-dimensional structures of the transmembrane domain, the Furin cleavage site, and the collagen domain have been shown for the first time. In this model, three Gly198 amino acid residues of the collagen domain are located around the trimeric THD. Changes resulting from mutations in the side chain volume and polarity with hydrophobic interactions of amino acid residues may prevent the oligomerization of THD and EDAR, thus impairing the receptor-binding ability and bioactivity of EDA.

In contrast to previous functional studies into the collagen domain (Schneider et al., 2001), we found that p.Gly198Glu and p.Gly198Ala impaired the receptor-binding activity of EDA1 proteins. In our study, we first constructed EDA1 expression vectors EDA1 S160 containing only 161 aa-391 aa as described before (Schneider et al., 2001). Coimmunoprecipitation showed the same result as previous studies in which collagen domain mutations had no direct affections on the receptor-binding ability. To reveal whether the full-length EDA1 protein has different impacts on receptor-binding activity, we then constructed full-length EDA1 expression vectors and found a different result. The full-length EDA1 expression vectors generate proteins more similar to in vivo proteins, and amino acids before S160 could theoretically influence the protein structure, which could affect the receptor-binding activity. Furthermore, PsiPred predicted that a huge difference occurred in the secondary structure of THD (250 aa-391 aa). This indicates that full-length protein is an alternative for functional studies if possible.

EDAR is activated by EDA1 and uses EDARADD as an adapter to build a signal-transducing complex that leads to NF-κB activation during the growth and development of ectodermal appendages. (Headon et al., 2001) (Smahi et al., 2002) The phenotypes of $C^{I\kappa B\alpha\Delta N}$ mice and Eda (*tabby*)- or Edar (*downless*)-deficient mice reveal that the Eda/Edar/NF-κB pathway regulates the developmental process and that gene mutations in this pathway result

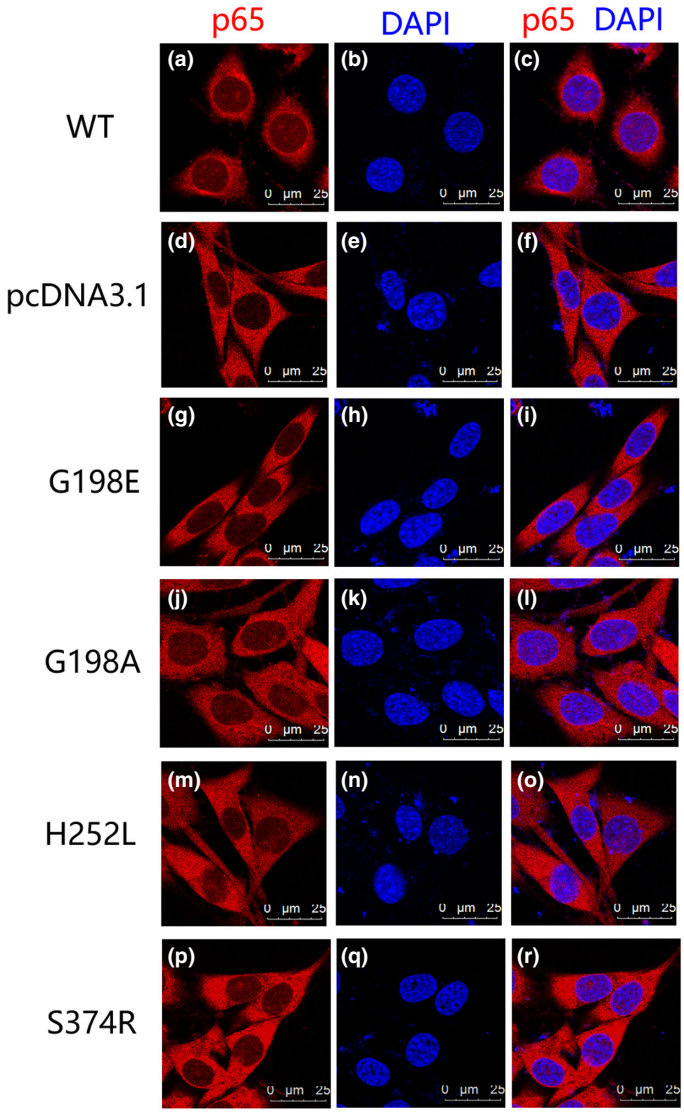

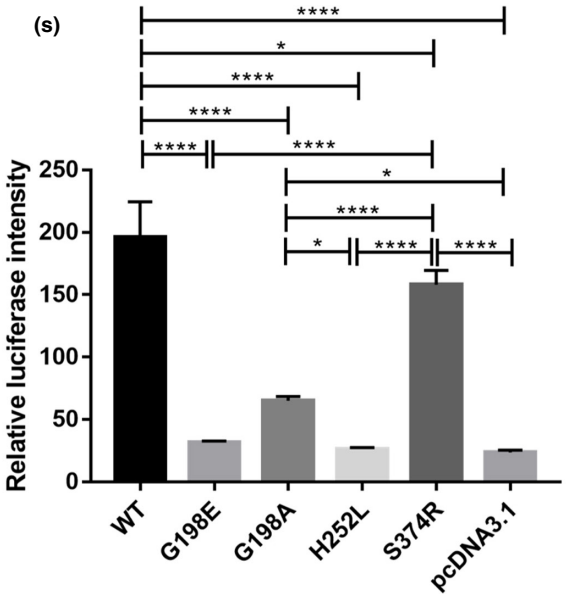

FIGURE 5 Transcriptional activation of NF-κB in LS8 cells expressing wild-type and mutant EDA1 proteins. (a–r) Immunofluorescence of NF-κB subunit p65 (p65, red; DAPI, blue) in LS8 cells transfected with wild-type EDA1: (a–c), pCR3.1 (d–f), HED-causing EDA1 mutants (d–o), and nonsyndromic tooth agenesis-causing EDA1 mutants (p–r). (s) Dual-luciferase assay revealed that mutant EDA1 proteins showed an obvious inhibitory effect on the transcriptional activation of NF-κB. $^{*}p < 0.05$; $^{**}p < 0.01$; $^{***}p < 0.001$.

in abnormalities in ectodermal appendages. (Schmidt-Ullrich et al., 2006) According to the dual luciferase assay and immunofluorescence results in this study, EDA mutations downregulate the transcriptional activation of NF-κB in LS8 cells, which is in keeping with earlier findings and indicates that p.Gly198Glu causes HED by interfering with NF-κB and its downstream signaling pathways.

In conclusion, we identified a novel mutation, p.Gly198Glu, in the collagen domain of EDA. Bioinformatics and functional studies results showed that mutations in this site affected the receptor binding and transcriptional activation of NF-κB, indicating that mutations in the collagen domain of EDA could result in HED by affecting the receptor-binding activity of EDA and transcriptional activity of NF-κB.

ACKNOWLEDGMENTS

We sincerely thank all the participants in this study. We gratefully acknowledge Dr. Malcolm L. Snead for generously providing us with LS8 cells.

AUTHOR CONTRIBUTIONS

Xingyu Liu: Conceptualization; data curation; formal analysis; writing original draft. Yuming Zhao: Conceptualization; data curation; writing review and editing. Junxia Zhu: Conceptualization; data curation; project administration; resources; supervision; writing review and editing.

FUNDING INFORMATION

This study was supported by the National Natural Science Foundation of China [grant number 81500828].

CONFLICT OF INTEREST

The authors declare that they have no known competing financial interests or personal relationships that could have appeared to influence the work reported in this paper.

ETHICS STATEMENT

Before the genetic studies, informed consent from the parents was obtained. The study was approved by the Peking University School of Stomatology Ethics Committee (approval number: PKUSSIRB-201628059).

ORCID

Xingyu Liu https://orcid.org/0000-0002-6050-0643

REFERENCES

Chen, L. S., Couwenhoven, R. I., Hsu, D., Luo, W., & Snead, M. L. (1992). Maintenance of amelogenin gene expression by transformed epithelial cells of mouse enamel organ. *Archives of Oral Biology*, *37*(10), 771–778. https://doi.org/10.1016/0003-9969(92)90110-t

Cluzeau, C., Hadj-Rabia, S., Jambou, M., Mansour, S., Guigue, P., Masmoudi, S., Bal, E., Chassaing, N., Vincent, M. C., Viot, G., Clauss, F., Manière, M. C., Toupenay, S., Le Merrer, M., Lyonnet, S., Cormier-Daire, V., Amiel, J., Faivre, L., de Prost, Y., … Smahi, A. (2011). Only four genes (*EDA1, EDAR, EDARADD, and WNT10A*) account for 90% of hypohidrotic/anhidrotic ectodermal dysplasia cases. *Human Mutation*, *32*(1), 70–72. https://doi.org/10.1002/humu.21384

Cui, C. Y., & Schlessinger, D. (2006). EDA signaling and skin appendage development. *Cell Cycle*, *5*(21), 2477–2483. https://doi.org/10.4161/cc.5.21.3403

Fan, H., Ye, X., Shi, L., Yin, W., Hua, B., Song, G., Shi, B., & Bian, Z. (2008). Mutations in the *EDA* gene are responsible for X-linked hypohidrotic ectodermal dysplasia and hypodontia in Chinese kindreds. *European Journal of Oral Sciences*, *116*(5), 412–417. https://doi.org/10.1111/j.1600-0722.2008.00555.x

Headon, D. J., Emmal, S. A., Ferguson, B. M., Tucker, A. S., Justice, M. J., Sharpe, P. T., Zonana, J., & Overbeek, P. A. (2001). Gene defect in ectodermal dysplasia implicates a death domain adapter in development. *Nature*, *414*(6866), 913–916. https://doi.org/10.1038/414913a

Keller, M. D., Petersen, M., Ong, P., Church, J., Risma, K., Burham, J., Jain, A., Stiehm, E. R., Hanson, E. P., Uzel, G., Deardorff, M. A., & Orange, J. S. (2011). Hypohidrotic ectodermal dysplasia and immunodeficiency with coincident *NEMO* and *EDA* mutations. *Frontiers in Immunology*, *2*, 61. https://doi.org/10.3389/fimmu.2011.00061

Kishore, U., & Reid, K. B. (1999). Modular organization of proteins containing C1q-like globular domain. *Immunopharmacology*, *42*(1–3), 15–21. https://doi.org/10.1016/s0162-3109(99)00011-9

Martínez-Romero, M. C., Ballesta-Martínez, M. J., López-González, V., Sánchez-Soler, M. J., Serrano-Antón, A. T., Barreda-Sánchez, M., Rodriguez-Peña, L., Martínez-Menchon, M. T., Frías-Iniesta, J., Sánchez-Pedreño, P., Carbonell-Meseguer, P., Glover-López, G., Guillén-Navarro, E., & GIEDE (Spanish multidisciplinary research group for ectodermal dysplasia). (2019). *EDA, EDAR, EDARADD and WNT10A* allelic variants in patients with ectodermal derivative impairment in the Spanish population. *Orphanet Journal of Rare Diseases*, *14*(1), 281. https://doi.org/10.1186/s13023-019-1251-x

Mues, G., Tardivel, A., Willen, L., Kapadia, H., Seaman, R., Frazier-Bowers, S., Schneider, P., & D'Souza, R. N. (2010). Functional analysis of Ectodysplasin-A mutations causing selective tooth agenesis. *European Journal of Human Genetics*, *18*(1), 19–25. https://doi.org/10.1038/ejhg.2009.127

Norderyd, J. (2012). Multidisciplinary treatment in children with ectodermal dysplasia. *Head & Face Medicine*, *8*(S1). https://doi.org/10.1186/1746-160x-8-s1-p5

Rahit, K., & Tarailo-Graovac, M. (2020). Genetic modifiers and rare Mendelian disease. *Genes (Basel)*, *11*(3). https://doi.org/10.3390/genes11030239

Reyes-Reali, J., Mendoza-Ramos, M. I., Garrido-Guerrero, E., Mendez-Catala, C. F., Mendez-Cruz, A. R., & Pozo-Molina, G. (2018). Hypohidrotic ectodermal dysplasia: Clinical and molecular review. *International Journal of Dermatology*, *57*(8), 965–972. https://doi.org/10.1111/ijd.14048

Schmidt-Ullrich, R., Tobin, D. J., Lenhard, D., Schneider, P., Paus, R., & Scheidereit, C. (2006). NF-kappaB transmits Eda A1/EdaR signalling to activate Shh and cyclin D1 expression, and controls

post-initiation hair placode down growth. *Development*, *133*(6), 1045–1057. https://doi.org/10.1242/dev.02278

Schneider, P., Street, S. L., Gaide, O., Hertig, S., Tardivel, A., Tschopp, J., Runkel, L., Alevizopoulos, K., Ferguson, B. M., & Zonana, J. (2001). Mutations leading to X-linked hypohidrotic ectodermal dysplasia affect three major functional domains in the tumor necrosis factor family member ectodysplasin-A. *The Journal of Biological Chemistry*, *276*(22), 18819–18827. https://doi.org/10.1074/jbc.M101280200

Shen, W., Wang, Y., Liu, Y., Liu, H., Zhao, H., Zhang, G., Snead, M. L., Han, D., & Feng, H. (2016). Functional study of Ectodysplasin-A mutations causing non-syndromic tooth agenesis. *PLoS One*, *11*(5), e0154884. https://doi.org/10.1371/journal.pone.0154884

Smahi, A., Courtois, G., Rabia, S. H., Doffinger, R., Bodemer, C., Munnich, A., Casanova, J. L., & Israel, A. (2002). The NF-kappaB signalling pathway in human diseases: From incontinentia pigmenti to ectodermal dysplasias and immune-deficiency syndromes. *Human Molecular Genetics*, *11*(20), 2371–2375. https://doi.org/10.1093/hmg/11.20.2371

Visinoni, A. F., Lisboa-Costa, T., Pagnan, N. A., & Chautard-Freire-Maia, E. A. (2009). Ectodermal dysplasias: Clinical and molecular review. *American Journal of Medical Genetics. Part A*, *149A*(9), 1980–2002. https://doi.org/10.1002/ajmg.a.32864

Wang, X., Zhang, Z., Yuan, S., Ren, J., Qu, H., Zhang, G., Chen, W., Zheng, S., Meng, L., Bai, J., du, Q., Yang, D., & Shen, W. (2020). A novel *EDA1* missense mutation in X-linked hypohidrotic ectodermal dysplasia. *Medicine (Baltimore)*, *99*(11), e19244. https://doi.org/10.1097/MD.0000000000019244

Wohlfart, S., Soder, S., Smahi, A., & Schneider, H. (2016). A novel missense mutation in the gene *EDARADD* associated with an unusual phenotype of hypohidrotic ectodermal dysplasia. *American Journal of Medical Genetics. Part A*, *170A*(1), 249–253. https://doi.org/10.1002/ajmg.a.37412

Zeng, B., Lu, H., Xiao, X., Zhou, L., Lu, J., Zhu, L., Yu, D., & Zhao, W. (2015). Novel *EDA* mutation in X-linked hypohidrotic ectodermal dysplasia and genotype-phenotype correlation. *Oral Diseases*, *21*(8), 994–1000. https://doi.org/10.1111/odi.12376

How to cite this article: Liu, X., Zhao, Y., & Zhu, J. (2022). A novel mutation in the collagen domain of EDA results in hypohidrotic ectodermal dysplasia by impacting the receptor-binding capability. *Molecular Genetics & Genomic Medicine*, *00*, e2119. https://doi.org/10.1002/mgg3.2119